2024 IEEE/RSJ International Conference on Intelligent Robots and Systems (IROS)
October 14-18, 2024. Abu Dhabi, UAE

Tunable Stiffness Glove for Tremor Suppression Based on 3D Printed Structured Fabrics

Yu Chen#, Junwei Li#, Xudong Yang, Yifan Wang*

Abstract— **Tremors, which are prevalent symptoms in both Parkinson's disease (PD) and essential tremor (ET), substantially diminish the quality of life for those affected. Traditional treatments, including pharmaceutical medications and invasive surgical procedures, often come with limitations and side effects, prompting the need for alternative solutions. In this paper, the Tunable Stiffness Glove (TSG) is developed as a non-invasive exoskeleton to suppress wrist tremors. By employing chain mail fabrics with tunable stiffness, the TSG permits natural wrist movement when in a soft state, while transitioning to a jammed state upon the application of negative pressure, effectively suppressing tremors in two directions. Evaluation of the TSG's efficacy was conducted through comprehensive three-point bending tests and human trials, utilizing commercial mechanical tester, inertial measurement unit (IMU), and electromyography (EMG) sensors. Weighing a mere 92 grams, the TSG demonstrated remarkable tremor suppression rates of 74.86%±5.52% (in the flexion-extension direction) and 66.80%±15.47% (in the adduction-abduction direction). Future enhancements aim to optimize the design for increased damping force and integrate sophisticated control strategies for improved user-exoskeleton interaction.**

I. INTRODUCTION

A tremor is characterized as an involuntary, rhythmic oscillation or shaking of a part of the body caused by periodic muscle contractions and relaxations [1]. Tremors can be categorized as physiological or pathological. Proper differentiation between the two types is crucial for appropriate medical intervention. While physiological tremors exist in almost everyone and will not affect daily life significantly, pathological tremors may lead to severe disabling conditions [2]. Parkinson's disease (PD) and essential tremor (ET) are the two most prevalent types of pathological tremors, especially among the elderly population. The incidence of ET among all age groups is estimated to be 0.9%, however, among older adults aged 65 years and above, the incidence rate increases significantly to 4.6% [3]. On the other hand, PD affects 0.3% of the population in industrialized countries, with the likelihood of occurrence increasing to 1% among individuals aged 60 years and above [4]. While not usually life-threatening, tremors can have a profound impact on the daily activities of patients. Tasks such as dressing, showering, or drinking water can become significantly more challenging and can ultimately lead to a further decline in the patient's quality of life.

Pharmaceutical medication is frequently utilized to address tremors associated with PD and ET [5]. However, its efficacy is often constrained, and it can lead to significant adverse effects such as allergic reactions, nausea, cardiac issues, and reduced white blood cell count [6]. Consequently, many individuals discontinue medical treatment due to intolerable side effects or perceived lack of effectiveness [7], [8]. Surgical interventions, including deep brain stimulation (DBS), are viable options for treating tremors. DBS is regarded as highly effective, with a potential efficacy rate of up to 90% [9]. However, this procedure entails risks of surgical complications such as disturbances in behavior and cognition, as it involves implanting electrodes into the brain. Further limitations of DBS therapy encompass risks of hemorrhage or infection, mechanical malfunctions, regular follow-up appointments, and expenses related to device implantation and battery replacements [10]–[13].

Given the limitations of traditional treatments, non-invasive exoskeletons have gained attention as a promising approach for tremor mitigation. These exoskeletons can be broadly classified into three categories—active systems, passive systems, and semi-active systems—depending on their mode of operation. [14], [15].

Active systems typically generate forces or torques counter to the involuntary tremors to offset the movement. Notable prototypes in this category include the Wearable Orthosis for Tremor Assessment and Suppression (WOTAS) [16], Tremor Alleviating Wrist Exoskeleton (TAWE) [17], Tremor Suppression Orthosis (TSO) [18], and Wearable Tremor Suppression Glove (WTSG) [19]. Many of these active systems are constructed with rigid frames, which tend to be heavy and bulky, with an average weight of 561 ± 467 g [5]. Additionally, they often lack the necessary flexibility to conform to the human body, potentially impeding natural movement rather than facilitating it.

Passive systems utilize shock absorbers or dissipators affixed to the tremor-affected body parts to suppress tremors. The first tremor-suppression device Viscous Beam was developed by Kotovsky et al. [20] in 1998. This wearable orthosis utilized viscous resistance to limit wrist motion and was designed to be sufficiently compact, allowing it to be worn discreetly beneath a shirt sleeve. The Task-Adjustable Passive Orthosis (TAPO), developed by Fromme et al. [21], is another notable contender in this category, renowned for its compact and lightweight design (33g). This orthosis utilizes air-filled structures to dampen wrist vibrations. While passive

This research was supported by A*STAR Singapore through RIE2025 MTC IRG award (M21K2c0118) and RIE2020 AME YIRG award (A2084c0162), and the NAP award (020482) from Nanyang Technological University.

# Contributed equally
* Corresponding author: Yifan Wang: yifan.wang@ntu.edu.sg
Yu Chen, Junwei Li, Xudong Yang and Yifan Wang are with the School of Mechanical and Aerospace Engineering, Nanyang Technological University, Singapore 639798.

systems boast the smallest average weight of 191 ± 137g and have demonstrated efficacy in prior research, their inherent passive mechanism may struggle to adapt to changes in tremor dynamics [1], [5].

Differing from the aforementioned systems, semi-active systems gauge tremor levels through sensor measurements and employ data to suppress movements by dynamically adjusting the system's impedance. Most of semi-active systems use magnetorheological (MR) fluid for damping forces, lighter and smaller than active systems. MR fluid can provide adequate damping force for tremor suppression, but heat from electromagnetic effects may alter viscosity and reduce sedimentation time. Maintenance and repair of MR fluid dampers can be cumbersome [22].

This paper presents a novel tunable stiffness glove designed for wrist tremor suppression, while also addressing muscle fatigue during prolonged weight-holding tasks. To enhance comfort and wearability, the glove incorporates structured fabrics with chain mail-type interlocking connections [23], offering variable stiffness by jamming the fabrics with negative pressure. Both the structured fabric and supporting components are fabricated using 3D printing technology. The effectiveness of the glove is validated using EMG and IMU sensors.

II. System Description

With the goal of developing a lightweight tremor-suppression exoskeleton that preserves natural wrist movement, the Tunable Stiffness Glove (TSG) comprises a tunable stiffness unit, soft covers, and non-stretchable belts, as shown in Table I. The schematic diagram of the TSG is depicted in Fig. 1.

TABLE I
Components of TSG System

Component Name	*Materials*	*Weight (g)*	*Quantity*
Tunable stiffness unit	Nylon (PA12), latex film, cotton cloth	50	1
Soft cover (hand)	Flexible resin (Formlabs)	18	1
Soft cover (wrist)	Flexible resin (Formlabs)	12	1
Non-stretchable belt (palm)	Cotton cloth	6	1
Non-stretchable belt (wrist)	Cotton cloth	6	1

Fig. 1(a) illustrates the prototype and three-dimensional model of the TSG worn on the right hand. For the tunable stiffness unit, chain mail fabrics [23] are chosen as the primary material, comprising two layers of interlocked particles. Within each layer, hollow octahedral particles are rotated 90° relative to each other and then connected via connecting trusses, thereby topologically interlocking all particles without forming solid connections. This unique construction reduces overall density while maximizing inter-element contact. Fabricated from high-strength lightweight nylon (PA12), the interlocked lattice is printed as a single piece using Selective Laser Sintering (SLS) technology, eliminating the need for additional supports while guaranteeing both light weight and ample mechanical strength.

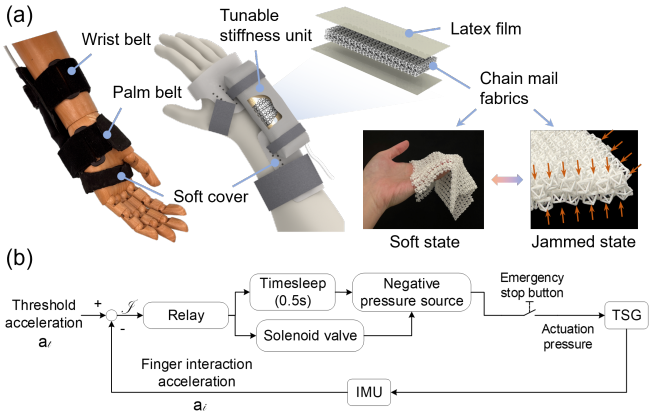

Fig. 1. System description. (a) Components of the tunable stiffness glove. (b) Closed-loop control strategy.

The structured fabrics exhibit tunable stiffness by transitioning from a soft state to a jammed state under the application of negative pressure. In the soft state, the chain mail fabrics function similarly to traditional fabrics, permitting relative sliding between layers and providing stretchability and flexibility for superior wrist conformability. However, under negative pressure, the boundary constraints cause the particles to move closer together, resulting in a more rigid and confined structure. Consequently, the bending stiffness of the tunable stiffness unit experiences a significant increase, effectively suppressing the tremors experienced by the wearer's wrist.

To ensure air-tight sealing, the two-layer chain mail fabrics are enveloped in latex films using silicone sealant, followed by wrapping with cotton cloth for comfort. To ensure the comfort of the TSG system, thermoplastic sheets were employed to create molds mirroring the human body surface via a rubbing technique. Following cooling and stiffening, these molds were 3D scanned, and the output files were processed to construct models of soft covers, which were ultimately 3D printed using flexible resin and an SLA printer. The tunable stiffness unit is affixed to the soft cover of the glove using non-stretchable belts, facilitating convenient replacement of a new tunable stiffness unit in the case of air leakage.

Fig 1(b) illustrates the control strategy of TSG system. An IMU sensor (LSM6DSOX + LIS3MDL) was positioned on the middle finger to capture real-time acceleration (a_i). This data was then transmitted to the microcontroller (Raspberry Pi Zero W) and compared to the predetermined threshold (a_t). When the real-time acceleration exceeded the threshold, indicating the onset of tremors in the wearer, the microcontroller sent an admittance signal (J) to the relay. Subsequently, the solenoid valve and negative pressure pump were activated sequentially. As a result, the tunable stiffness unit stiffened to suppress the tremors. Once the tremors ceased and the real-time acceleration fell below the threshold, the relay was deactivated, and the negative pressure was released through the solenoid valve. Consequently, the tunable stiffness unit returned to its soft state, allowing for free wrist

movements.

III. Experimental Protocol

A. Damping Force Test

To assess the stiffness variation of the tunable stiffness unit in different directions and determine the adequacy of the damping force for tremor suppression on human wrists, three-point bending tests were conducted using a mechanical tester (AG-X plus, SHIMADZU). The mechanical tester was equipped with force sensors (range: 0–10 kN, sensitivity: 0.01 N), and travel sensors (range: 0-1150 mm, sensitivity: 0.001 mm). The tunable stiffness unit sample was connected to the pressure control module via air tubes and positioned at the fixed end of the tester. Subsequently, the sample was indented by the tester for 15 mm, with the indenting position chosen to align with the coverage area of the tunable stiffness unit on the wrist. To achieve quasi-static conditions, the loading rate was set to 15 mm/min.

The TSG system was designed to suppress wrist tremors in two directions: extension-flexion and adduction-abduction. Consequently, the three-point bending tests were conducted along these respective directions.Due to the symmetrical distribution of the tunable stiffness unit's structure in both the extension-flexion and adduction-abduction directions, it was deemed adequate to assess bending performance in a single bending direction per test series. The stiffness of the unit, governed by the confining pressure, was evaluated at negative pressures of 0 kPa, 20 kPa, 40 kPa, 60 kPa, and 80 kPa. Each pressure condition was tested in triplicate, and the results were averaged for analysis. Standard deviations were calculated to assess the variability and reliability of the measurements.

B. Tremor Suppression Test

Three healthy male participants (P1: 24 years old, 180 cm, 80 kg; P2: 28 years old, 170 cm, 62 kg; P3: 27 years old, 175 cm, 65 kg) were recruited for the tremor suppression test. Upon receiving detailed information about the study, participants provided their informed consent. The experiments conducted at Nanyang Technological University were reviewed and approved by the institutional ethics committee. All experimental procedures were carried out in accordance with the ethical standards set forth in the Helsinki Declaration.

Throughout the experiment, wrist tremors in both extension-flexion and adduction-abduction, with inactivated and activated TSG system, were assessed. Three repeated trials were conducted for each condition. During each trial, participants maintained static posture for the first 5 seconds, followed by wrist vibration at their natural frequencies for 15 seconds (observed to range between 2-4 Hz), resulting in a total trial duration of 20 seconds. Two Trigno Avanti sensors (Delsys Incorporated, USA) were positioned on the participants' middle finger and brachioradialis muscle separately to record EMG and acceleration data. The EMG signal was sampled at a rate of 1926 Hz, while the acceleration data was sampled at 148 Hz. Participants were instructed to keep their fingers unbent to avoid relative acceleration between the fingers and the wrist.

C. Fatigue Test

According to previous research, a significant drawback of traditional invasive treatments like functional electrical stimulation (FES) is the potential for rapid muscle fatigue [24], [25]. Therefore, two participants (P1: 24 years old, 180 cm, 80 kg; P2: 28 years old, 170 cm, 62 kg) were recruited to test muscle fatigue during prolonged wear of the TSG system. The test lasted for 6 minutes, during which a 1 kg load was placed on the participants' right hand after the first five seconds. Participants were instructed to maintain their hand, wrist, and forearm horizontally with the load for the remainder of the time while wearing both the inactivated and activated TSG system. One Trigno Avanti sensor was positioned on the participants' brachioradialis muscle to record EMG data, as this muscle is activated to maintain wrist posture. The sample rate was 1926 Hz. To eliminate the influence of fatigue between trials, participants were required to rest for at least 30 minutes between every two trials.

IV. Results and Discussions

A. Mechanical Property of Tunable Stiffness Unit

In reference to previous study [23], force-displacement curves of the tunable stiffness unit was obtained via three-point bending tests, as shown in Fig. 2(a) to (b).

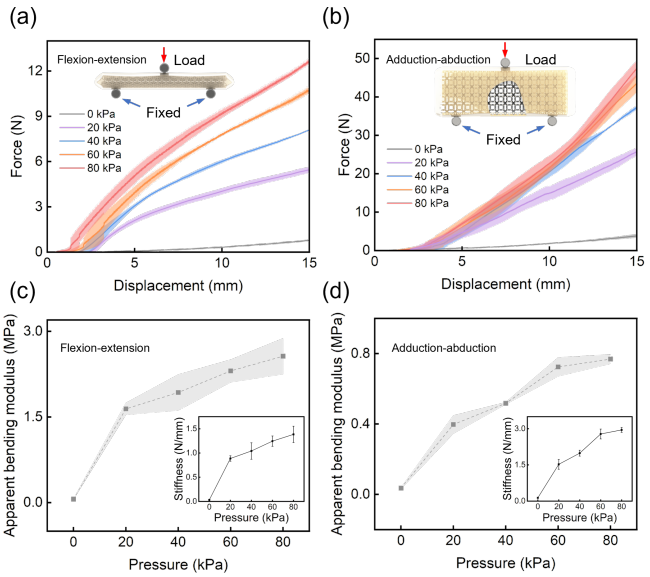

Fig. 2. Bending test of chain mail fabrics under different confining pressures. Measured force-displacement curves in the extension-flexion (a) and adduction-abduction (b) direction. Apparent bending modulus and stiffness in the extension-flexion (c) and adduction-abduction (d) direction. The colored lines denote average values, and the shaded area and error bars represent the standard deviation across three separate tests.

Fig. 2(c) to (d) depict the stiffness and apparent bending modulus, as derived from the initial linear region of the force-displacement curves in both the extension-flexion and adduction-abduction directions. These measures were used

to quantify changes in the mechanical properties of the tunable stiffness unit under different confining pressures. The stiffness and apparent bending modulus can be calculated as follows [26]–[28]:

$$K = \frac{F}{d}$$
$$E = \frac{KL^3}{4bh^3} \quad (1)$$

Where K is the stiffness of the tunable stiffness unit sample, F and d are the force and displacement obtained from the mechanical tester, and L, b and h are the length, width and height of the sample, respectively, prior to the bending test..

As confining pressure increased from 0 kPa to 80 kPa, the apparent bending modulus demonstrated a significant enhancement in the extension-flexion direction, rising from approximately 0.0598 MPa to 2.56 MPa. Consequently, under a confining pressure of 80 kPa, the maximum damping force reached approximately 12.6 N, surpassing that of many other prototypes [15], [29] and proving sufficient for wrist tremor suppression. Same results can be observed in the adduction-abduction direction. The apparent bending modulus increased from 0.0354 MPa to 0.769 MPa, achieving a maximum damping force of 47.4 N. Notably, the damping force exhibited a substantial rise as confining pressure increased from 0 kPa to 20 kPa. In contrast, the increase in damping force was minimal when the pressure was elevated from 60 kPa to 80 kPa. Moreover, achieving a confining pressure of 80 kPa requires a bulky negative pressure pump operating at least 24 V, making it impractical for ensuring the portability and lightweight nature of the system. Consequently, a confining pressure of 60 kPa was chosen as the standard working pressure, as it can be achieved using a compact 9V vacuum pump (ϕ24*59.5 mm, 40g). Subsequent tests were conducted using this standard pressure. For patients with severe tremors, the working pressure may be adjusted up to 80 kPa; however, this adjustment would unavoidably result in an increase in both the size and weight of the entire system.

B. Efficiency of Tremor Suppression

To measure the effectiveness of the TSG system in suppressing tremors, EMG and IMU sensors were employed to gauge muscle activation and acceleration, as depicted in Fig. 3.

Fig. 3(a) to (b) depict the tremor range of the wearer's wrist under different conditions. In the extension-flexion direction, under the soft state, the tremor reached a range of about 100 degrees, while it was approximately 32 degrees under the jammed state. Similarly, in the adduction-abduction direction, under the soft state, the tremor reached a range of about 90 degrees, while it was approximately 30 degrees under the jammed state. This reduction signifies the effectiveness of the TSG system in constraining wrist posture and suppressing wearer tremors.

The data collected by the EMG and IMU sensors further confirm the effectiveness of the TSG system. Referring to the previous studies [30], [31], the EMG signal's amplitude

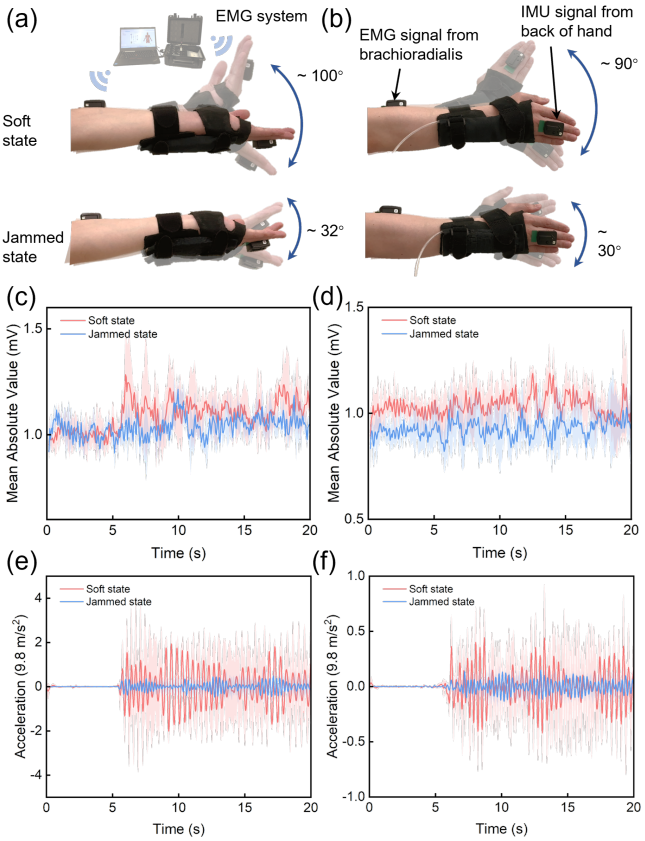

Fig. 3. Tremor suppression tests of P1 wearing TSG system. (a) Tremors along extension-flexion direction. (b) Tremors along abduction-adduction direction. (c) Mean absolute value of EMG signals of tremors along extension-flexion direction. (d) Mean absolute value of EMG signals of tremors along abduction-adduction direction. (e) IMU signals of tremors along extension-flexion direction. (f) IMU signals of tremors along abduction-adduction direction.

reflects the activation level of the targeted muscle, with the mean absolute value (MAV) being the most commonly used indicator of EMG amplitude in the time domain. However, several processing steps are necessary from the raw signals, including filtering, whitening, amplitude demodulation, smoothing, and relinearization [32]. Therefore, a bandpass second-order Butterworth filter was employed to remove noise such as motion artifacts, power line interference, and electronic noise. Subsequently, MAV was calculated as follows:

$$\text{MAV} = \frac{1}{N}\sum_{i=1}^{N}|x_i| \quad (2)$$

Where x_i is the ith sample of EMG signal, and N is the number of samples in the epoch. After acquiring the MAV, the demodulated samples were time-averaged to produce amplitude estimates, employing a sliding window technique.

Fig. 3(c) to (d) illustrate the MAV of brachioradialis muscle derived from the raw EMG signal during the tremor test in both extension-flexion and adduction/abduction directions, and Fig. 3(e) to (f) depicts the corresponding acceleration

from back of hand. It is evident that the MAV remained comparable when wearing the TSG under both the soft and jammed states. This suggests that the activation level of the brachioradialis muscle remained consistent, indicating that participants did not intentionally force their wrist to tremor at different amplitudes. Meanwhile, the acceleration exhibited a notable decrease after activating the TSG. This indicates that, with similar muscle activation, the tremors were effectively suppressed by the TSG under the jammed state. To quantify the efficiency of TSG using acceleration data, tremor suppression efficiency η_{TSG} was introduced as follows [14]:

$$\eta_{TSG} = \left(1 - \frac{Acc(i,J)}{Acc(i,S)}\right) \times 100\%, \quad i = \alpha, \beta \tag{3}$$

Where $Acc(i,J)$ is the maximum acceleration in the ith direction under jammed state, $Acc(i,S)$ is the maximum acceleration in the ith direction under soft state, α and β are the direction along flexion-extension and adduction-abduction.

It can be calculated that while working at 60 kPa, η_{TSG} in above two directions are 74.86%±5.52% and 66.80%±15.47%, respectively. Based on these results, it can be concluded that the TSG system is effective in suppressing wrist tremors in both the extension-flexion and adduction-abduction directions.

C. Fatigue Performance

Since the TSG was designed to assist in daily activities, its long-term performance should be evaluated to determine if the system imposes additional burden on the human body. A Trigno Avanti sensor was attached on the participants' brachioradialis muscle during the 6-minute fatigue test, as shown in Fig. 4.

Muscle fatigue performance can be assessed in the frequency domain of the EMG signal, where fatiguing contractions cause a shift in the power spectrum density (PSD) towards lower frequencies [33]. Therefore, the raw EMG data were initially subjected to a second-order Butterworth bandpass filter. Following this, the signal was converted from the time domain to the frequency domain using Fast Fourier Transform (FFT), as shown in Fig. 4(b). It is noticeable that when wearing the TSG in a soft state, the EMG signal demonstrates more components distributed in the low-frequency range, suggesting a higher level of fatigue.

For a clearer comparison, biomechanical parameters were chosen to quantify the frequency of EMG signals. The mean frequency (MNF) and median frequency (MDF) are commonly used parameters to represent the change of frequency as muscles fatigue, and can be calculated as follows [30]:

$$f_{\text{mean}} = \frac{\int_0^{f_s/2} f P(f) df}{\int_0^{f_s/2} f P(f) df}, \tag{4}$$

$$\int_0^{f_{\text{med}}} P(f)\mathrm{d}f = \frac{1}{2}\int_0^{f_s/2} P(f)\mathrm{d}f \tag{5}$$

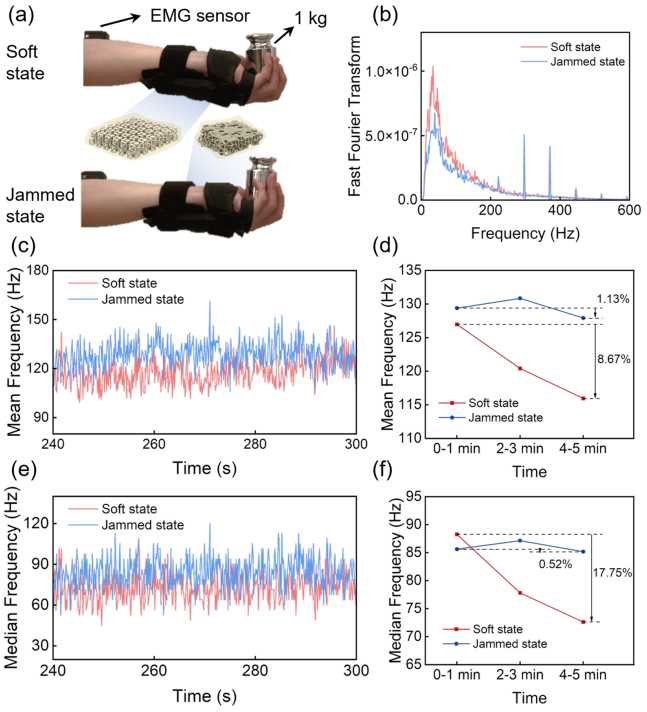

Fig. 4. Muscle fatigue tests of P2 wearing TSG system. (a) Setup of 6-minute holding experiment. (b) Fast Fourier transform of EMG signals. (c) Mean frequency of EMG signals during the fifth minute. (d) Tendency of mean frequency during fatigue tests. (e) Median frequency of EMG signals during the fifth minute. (f) Tendency of median frequency during fatigue tests.

Where f_{mean} is the mean frequency of the EMG signal, f_s is the sampling frequency, f_{med} is the median frequency, and $P(f)$ is the power spectrum density of the signal.

Fig. 4(c) illustrates the frequency-time curves of MNF during fatigue tests, both with the TSG deactivated and activated. Due to the large volume of data, only frequencies from the fifth minute (240 to 300s) were extracted for analysis. The MNF was also smoothed using a sliding window. It is evident that the MNF was higher when the TSG was activated, indicating a lower fatigue level of the brachioradialis muscle. However, the change of MNF over time is not clearly presented. Therefore, the mean values of MNF during 0 to 1, 2 to 3, and 4 to 5 minutes were calculated, as depicted in Fig. 4(d). Under the soft state, the MNF dropped by 8.67% during the test, whereas under the jammed state, it only decreased by 1.13%. Similar trends are observed in the MDF data, as depicted in Figures 4(e) to (f). Under the soft state, the MDF dropped by 17.75% during the test, while under the jammed state, it only decreased by 0.52%. These results suggest that the TSG not only imposes no additional burden on the human body but also assists in holding tasks as a supportive exoskeleton. Holding tasks are commonplace in daily life, such as drinking water, holding a book to read, or carrying a baby, highlighting the TSG's potential as a promising solution for long-term tremor suppression.

TABLE II
PARAMETERS OF EXISTING SYSTEMS

Name	*Suppression Mechanism*	*Weight (g)*	*DoF*	*Damping Force*	*Efficiency*
WOTAS [16]	Active	850	3 (EFE, FAA, WFE)	-	40%
TSO [18]	Active	1700	1 (EFE)	0.62 ± 0.04 Nm	94.4%
TAWE [17]	Active	485	2 (WFE,WAA)	-	-
EFB [34]	Semi-active	942	1 (EFE)	2.2 Nm	88%
VSW-Exo [14]	Semi-active	443 - 589	3 (WFE, WAA, WPS)	18.07 - 29.71 N (WFE) 7.3 - 65.97 N (WAA) 0.93 Nm (WPS)	64.11% (WFE) 67.24% (WAA) 64.45% (WPS)
WTSE [15]	Semi-active	262.13	1 (WFE)	8 N	60.39% (Acceleration) 55.07% (Angular velocity)
SETS [29]	Semi-active	255	3 (WFE, WAA, WPS)	11 N	61.39% (Acceleration) 56.22% (Angular velocity)
Viscous beam [20]	Passive	260	1 (WFE)	0.39 Nm	-
Air dashpots [35]	Passive	-	3 (EFE, WFE, WAA)	-	20% - 62%
TAPO [21]	Passive	33	2 (WFE, WAA)	0.3 Nm	78%
TSG (This work)	Semi-active	92	2 (WFE, WAA)	12.6 N	74.86% ± 5.52% (WFE) 66.80% ± 15.47% (WAA)

EFE: elbow flexion-extension, FAA: forearm adduction-abduction, WFE: wrist flexion-extension, WAA: wrist adduction-abduction, WPS: wrist pronation-supination

D. Comparison to Existing Systems

Given that the field of rehabilitation exoskeletons is still emerging, there have been relatively few proposed systems specifically designed for wrist tremor suppression. Table II compares the technical parameters of existing wrist tremor suppression systems with the TSG proposed in this paper. The overall efficiency of the TSG is approximately 70%, comparable to TAPO developed by Fromme et al. [21]. However, the semi-active mechanism makes the TSG more adaptable to different daily scenarios. Furthermore, the TSG system can generate a damping force exceeding 10 N at 60 kPa (12.6 N at 80 kPa) using a compact vacuum pump operating at 9 V. This force surpasses that of most magnetorheological (MR) fluid dampers while requiring lower energy consumption compared to motor-based systems. Moreover, most existing wrist tremor suppression systems cover from the wearer's hand to the elbow, restricting the natural movement of the forearm. Their size and weight make them impractical to be concealed under clothing, potentially causing disease-related shame during daily use. In contrast, the TSG system is lightweight, compact, and resembles a normal glove, enhancing its acceptability for long-term treatment.

V. CONCLUSIONS

In this study, a novel wrist tremor suppression exoskeleton utilizing chain mail fabrics is developed. The adjustable stiffness characteristic of these fabrics enables unrestricted wrist movement in their soft state and effectively suppresses tremors in two directions upon the application of negative pressure. Three-point bending tests were conducted to assess the system's ability to adjust stiffness, and the damping force was measured under various confining pressures. Commercial IMU and EMG sensors were employed to evaluate the performance of the Tremor Suppression Glove (TSG) during human trials. The EMG and IMU signals were then analyzed to validate the system's effectiveness. Additionally, fatigue tests were conducted to ensure that the TSG system does not impose excessive strain on the user. Future improvement of the TSG system will focus on optimizing the design of the adjustable stiffness unit to achieve higher damping force under similar confining pressures. More sophisticated and intelligent control strategies will also be implemented to enhance the interaction between users and the exoskeleton.

ACKNOWLEDGMENT

The authors wish to express their sincere appreciation to Prof. Kong Pui Wah and her team for graciously providing the Trigno system utilized in our experiments. Additionally, heartfelt thanks are extended to the participants who generously volunteered their time and effort to partake in the human trials essential for this study. Their invaluable support and assistance greatly contributed to the successful culmination of this research endeavor.

REFERENCES

[1] K. P. Bhatia, P. Bain, N. Bajaj, R. J. Elble, M. Hallett, E. D. Louis, J. Raethjen, M. Stamelou, C. M. Testa, G. Deuschl *et al.*, "Consensus statement on the classification of tremors. from the task force on tremor of the international parkinson and movement disorder society," *Movement Disorders*, vol. 33, no. 1, pp. 75–87, 2018.

[2] J. S. Lora-Millan, G. Delgado-Oleas, J. Benito-León, and E. Rocon, "A review on wearable technologies for tremor suppression," *Frontiers in neurology*, vol. 12, p. 700600, 2021.

[3] E. D. Louis and J. J. Ferreira, "How common is the most common adult movement disorder? update on the worldwide prevalence of essential tremor," *Movement Disorders*, vol. 25, no. 5, pp. 534–541, 2010.

[4] L. M. De Lau and M. M. Breteler, "Epidemiology of parkinson's disease," *The Lancet Neurology*, vol. 5, no. 6, pp. 525–535, 2006.

[5] H. S. Nguyen and T. P. Luu, "Tremor-suppression orthoses for the upper limb: current developments and future challenges," *Frontiers in Human Neuroscience*, vol. 15, p. 622535, 2021.

[6] J. A. Gallego, E. Rocon, and J. L. Pons, "Estimation of instantaneous tremor parameters for fes-based tremor suppression," in *2010 IEEE International Conference on Robotics and Automation*. IEEE, 2010, pp. 2922–2927.

[7] R. J. O'Connor and M. U. Kini, "Non-pharmacological and non-surgical interventions for tremor: a systematic review," *Parkinsonism & related disorders*, vol. 17, no. 7, pp. 509–515, 2011.

[8] N. L. Diaz and E. D. Louis, "Survey of medication usage patterns among essential tremor patients: movement disorder specialists vs. general neurologists," *Parkinsonism & related disorders*, vol. 16, no. 9, pp. 604–607, 2010.

[9] R. Elble and G. Deuschl, "Milestones in tremor research," *Movement Disorders*, vol. 26, no. 6, pp. 1096–1105, 2011.

[10] J. Hubble, K. Busenbark, S. Wilkinson, R. Penn, K. Lyons, and W. Koller, "Deep brain stimulation for essential tremor," *Neurology*, vol. 46, no. 4, pp. 1150–1153, 1996.

[11] Y. Katayama, T. Kano, K. Kobayashi, H. Oshima, C. Fukaya, and T. Yamamoto, "Difference in surgical strategies between thalamotomy and thalamic deep brain stimulation for tremor control," *Journal of neurology*, vol. 252, pp. iv17–iv22, 2005.

[12] S. Miocinovic, S. Somayajula, S. Chitnis, and J. L. Vitek, "History, applications, and mechanisms of deep brain stimulation," *JAMA neurology*, vol. 70, no. 2, pp. 163–171, 2013.

[13] M. I. Hariz, S. Rehncrona, N. P. Quinn, J. D. Speelman, and C. Wensing, "Multicenter study on deep brain stimulation in parkinson's disease: an independent assessment of reported adverse events at 4 years," *Movement disorders: official journal of the Movement Disorder Society*, vol. 23, no. 3, pp. 416–421, 2008.

[14] G. Wang, H. Wang, W. Gao, X. Yang, and Y. Wang, "Jamming enabled variable stiffness wrist exoskeleton for tremor suppression," *IEEE Robotics and Automation Letters*, 2023.

[15] A. Yi, A. Zahedi, Y. Wang, U.-X. Tan, and D. Zhang, "A novel exoskeleton system based on magnetorheological fluid for tremor suppression of wrist joints," in *2019 IEEE 16th International Conference on Rehabilitation Robotics (ICORR)*. IEEE, 2019, pp. 1115–1120.

[16] E. Rocon, J. M. Belda-Lois, A. Ruiz, M. Manto, J. C. Moreno, and J. L. Pons, "Design and validation of a rehabilitation robotic exoskeleton for tremor assessment and suppression," *IEEE Transactions on neural systems and rehabilitation engineering*, vol. 15, no. 3, pp. 367–378, 2007.

[17] J. Wang, O. Barry, A. J. Kurdila, and S. Vijayan, "On the dynamics and control of a full wrist exoskeleton for tremor alleviation," in *Dynamic Systems and Control Conference*, vol. 59155. American Society of Mechanical Engineers, 2019, p. V002T27A008.

[18] G. Herrnstadt, M. J. McKeown, and C. Menon, "Controlling a motorized orthosis to follow elbow volitional movement: tests with individuals with pathological tremor," *Journal of NeuroEngineering and Rehabilitation*, vol. 16, pp. 1–14, 2019.

[19] Y. Zhou, M. E. Jenkins, M. D. Naish, and A. L. Trejos, "Development of a wearable tremor suppression glove," in *2018 7th IEEE International Conference on Biomedical Robotics and Biomechatronics (Biorob)*. IEEE, 2018, pp. 640–645.

[20] J. Kotovsky and M. J. Rosen, "A wearable tremor-suppression orthosis," *Journal of rehabilitation research and development*, vol. 35, pp. 373–387, 1998.

[21] N. P. Fromme, M. Camenzind, R. Riener, and R. M. Rossi, "Design of a lightweight passive orthosis for tremor suppression," *Journal of neuroengineering and rehabilitation*, vol. 17, pp. 1–15, 2020.

[22] Y. M. Khedkar, S. Bhat, and H. Adarsha, "A review of magnetorheological fluid damper technology and its applications," *Int. Rev. Mech. Eng*, vol. 13, no. 4, pp. 256–264, 2019.

[23] Y. Wang, L. Li, D. Hofmann, J. E. Andrade, and C. Daraio, "Structured fabrics with tunable mechanical properties," *Nature*, vol. 596, no. 7871, pp. 238–243, 2021.

[24] N. P. Fromme, M. Camenzind, R. Riener, and R. M. Rossi, "Need for mechanically and ergonomically enhanced tremor-suppression orthoses for the upper limb: a systematic review," *Journal of neuroengineering and rehabilitation*, vol. 16, pp. 1–15, 2019.

[25] M. Javidan, J. Elek, and A. Prochazka, "Attenuation of pathological tremors by functional electrical stimulation ii: clinical evaluation," *Annals of biomedical engineering*, vol. 20, pp. 225–236, 1992.

[26] C. Zweben, W. Smith, and M. Wardle, "Test methods for fiber tensile strength, composite flexural modulus, and properties of fabric-reinforced laminates," in *Composite Materials: Testing and Design (Fifth Conference)*. ASTM International, 1979.

[27] X. Yang, M. Liu, B. Zhang, Z. Wang, T. Chen, Y. Zhou, Y. Chen, K. J. Hsia, and Y. Wang, "Hierarchical tessellation enables programmable morphing matter," *Matter*, 2023.

[28] X. Yang, M. Liu, T. Chen, Y. Chen, and Y. Wang, "Tunable mechanics of architectured composites from particle assemblies," *Extreme Mechanics Letters*, vol. 67, p. 102121, 2024.

[29] A. Zahedi, B. Zhang, A. Yi, and D. Zhang, "A soft exoskeleton for tremor suppression equipped with flexible semiactive actuator," *Soft robotics*, vol. 8, no. 4, pp. 432–447, 2021.

[30] M. Cifrek, V. Medved, S. Tonković, and S. Ostojić, "Surface emg based muscle fatigue evaluation in biomechanics," *Clinical biomechanics*, vol. 24, no. 4, pp. 327–340, 2009.

[31] N. J. Jarque-Bou, J. L. Sancho-Bru, and M. Vergara, "A systematic review of emg applications for the characterization of forearm and hand muscle activity during activities of daily living: results, challenges, and open issues," *Sensors*, vol. 21, no. 9, p. 3035, 2021.

[32] E. A. Clancy, E. L. Morin, and R. Merletti, "Sampling, noise-reduction and amplitude estimation issues in surface electromyography," *Journal of electromyography and kinesiology*, vol. 12, no. 1, pp. 1–16, 2002.

[33] J. H. Viitasalo and P. V. Komi, "Signal characteristics of emg during fatigue," *European journal of applied physiology and occupational physiology*, vol. 37, pp. 111–121, 1977.

[34] G. Herrnstadt and C. Menon, "On-off tremor suppression orthosis with electromagnetic brake," *International Journal of Mechanical Engineering and Mechatronics*, vol. 1, no. 2, pp. 7–24, 2012.

[35] M. Takanokura, R. Sugahara, N. Miyake, K. Ishiguro, T. Muto, and K. Sakamoto, "Upper-limb orthoses implemented with air dashpots for suppression of pathological tremor in daily activites," in *ISB conference July*, 2011, pp. 3–4.